Malaysian Journal of Analytical Sciences (MJAS)
Published by Malaysian Analytical Sciences Society

MOLYBDENUM DISULFIDE FOR PHOTOCATALYTIC DEGRADATION OF METHYLENE BLUE UNDER FLUORESCENT LIGHT

(Molybdenum Disulfida Untuk Fotokatalitik Degradasi Metilena Biru Di Bawah Cahaya Pendarfluor

Siti Nor Atika Baharin[1, 2], Nurul Izzah Hashim[1], Izyan Najwa Mohd Norsham[1], and Kavirajaa Pandian Sambasevam[1,3*]

[1]Advanced Material for Environmental Remediation (AMER) Research Group,
Faculty of Applied Sciences,
Universiti Teknologi MARA, Cawangan Negeri Sembilan, Kampus Kuala Pilah,
72000 Kuala Pilah, Negeri Sembilan, Malaysia
[2]Advanced Biomaterials & Carbon Development (ABCD),
Universiti Teknologi MARA, 40450, Shah Alam, Selangor, Malaysia
[3]Electrochemical Material and Sensor (EMas) Group,
Universiti Teknologi MARA,
40450 Shah Alam, Selangor, Malaysia

[*]Corresponding author: kavirajaa@live.com

Received: 25 September 2022; Accepted: 20 May 2023; Published: 22 August 2023

Abstract

This work underlined the fluorescent light-driven photocatalytic degradation of methylene blue by using cauliflower-like molybdenum disulfide (MoS_2). In this study, molybdenum disulfide (MoS_2) was synthesized by using Teflon-stainless steel autoclave via the hydrothermal method. The synthesized MoS_2 were comprehensively characterized using Fourier transform infrared (FTIR), UV-visible spectroscopy, X-ray diffraction (XRD), scanning electron microscopy (SEM), and thermal gravimetry analysis (TGA). The characterization studies reveal that the composites have been successfully synthesized in which a black precipitate was obtained. Degradation of methylene blue was conducted using the synthesized MoS_2 under fluorescent light using response surface methodology (RSM) of three-factor-three-level Box-Behnken design (BBD). The parameters studied were MoS_2 weight loading, contact time under fluorescent light, and methylene blue pH value. The most effective parameter observed in the degradation of methylene blue were weight loading, followed by contact time and pH. The results showed that the optimum condition for the degradation were with the parameters of 15mg of MoS_2 weight loading, with pH 6.5 methylene blue, has the highest degradation percentage 99.93% with 120 minutes exposed time under fluorescent light for degradation.

Keywords: molybdenum disulfide, photocatalytic degradation, methylene blue, response surface methodology, Box-Behnken

Abstrak

Penyelidikan ini menggariskan degradasi fotokatalitik dipacu cahaya pendarfluor biru metilena dengan menggunakan molibdenum disulfida (MoS_2) yang berbentuk kobis bunga. Dalam kajian ini, molibdenum disulfida (MoS_2) telah disintesis dengan menggunakan autoklaf keluli tahan karat Teflon melalui kaedah hidroterma. MoS_2 yang disintesis telah dicirikan secara komprehensif menggunakan inframerah transformasi Fourier (FTIR), spektroskopi boleh dilihat UV, pembelauan sinar-X (XRD), mikroskop elektron pengimbasan (SEM), dan analisis gravimetri terma (TGA). Kajian pencirian mendedahkan bahawa komposit telah berjaya disintesis di mana mendakan hitam diperolehi. Degradasi metilena biru telah dijalankan menggunakan MoS_2 yang disintesis di bawah cahaya pendarfluor menggunakan metodologi permukaan tindak balas (RSM) reka bentuk Box-Behnken (BBD) tiga faktor-tiga peringkat. Parameter yang dikaji ialah pemuatan berat MoS_2, masa sentuhan di bawah cahaya pendarfluor, dan nilai pH biru metilena. Parameter paling berkesan yang diperhatikan dalam degradasi metilena biru ialah pemuatan berat, diikuti dengan masa sentuhan dan pH. Keputusan menunjukkan bahawa keadaan optimum untuk degradasi adalah dengan parameter 15mg beban berat MoS2, dengan pH 6.5 metilena biru, mempunyai peratusan degradasi tertinggi 99.93% dengan 120 minit masa terdedah di bawah cahaya pendarfluor untuk degradasi.

Kata kunci: molibdenum disulfida, degradasi fotokatalitik, biru metilena, metodologi permukaan tindak balas, Box-Behnken

Introduction

With the advancements of the textile industry in recent years, an increasing number of dyes, like methylene blue have been developed. According to the World Bank analysis, textile dyeing and finishing operations accounted for over 20% of global industrial water contamination [1]. Synthetic dyes are widely utilised in a variety of industries, including food, textile, paper, rubber, plastics, cosmetics and pharmaceuticals. These manufacturers dumped massive amounts of effluent into waterways with no prior treatment. These discharges are a significant source of contamination and contributed to the deterioration of human health and environmental [2]. Dyes also have an impact on aquatic life by interfering with the photosynthesis process of aquatic plants, causing eutrophication and causing disturbance [3, 4]. Due to methylene blue (MB) properties of limited biodegradability, traditional treatment methods, such as the physical-chemical approach is ineffective [5]. The conventional water-treatments approaches applied in individual or combined systems may be applicable to treat mild polluted waste, unfortunately, all these methods do not comprehensively eliminate the pollutant and the detrimental sludge remains after the treatment. Recently, photocatalytic degradation became one of the efficient techniques to degrade pollutants [6, 7].

Photocatalytic degradation is a technique that utilize light source and forms electron-hole which produce radicals that can convert contaminant to safe and less poisonous substances. Special feature of photocatalytic degradation is that it can degrade organic pollutants that has high photochemical stability by effectively utilize light irradiation [8]-[9]. According to Poorsajadi et al., 88% of MB was degraded by using CuO/Bi_2O_3 nanocomposite as photocatalyst under UV irradiation [10]. Meanwhile, γ -Fe_3/Fe_3O_4/ SiO_2 (Ar modified) composite successfully synthesized and degraded MB in 120 min with 87.5% of degradation [11]. On the other hand, 99% of MB was removed by only 4 min by using Ternary $MoS_2/Bi_2S_3/TiO_2$ heterostructure as photocatalyst under simulated solar irradiation as the light source [12]. Molybdenum disulfide (MoS_2) can be used in degradation of organic pollutant. MoS_2 is a crystal structure that comprised S-Mo-S layers that are poorly coupled, whereby a Mo atom layer is in between two S atom layers. A spontaneously existing layered solid, namely MoS_2, seeks uses for production in either its bulk or dispersed forms. The discrete sandwiched S-Mo-S layers are fused together by poor Van der Waals interactions in hexagonally packed frameworks. These layers may shift efficiently towards each other, which enables MoS_2 as a commonly applied dry lubricant. The Van der Waals gaps between the layers are responsible for its properties like anisotropy, good catalytic property, chemical inertness, photo corrosion resistance, optical properties and biological applications [13]-[15]. Due to its distinct layered properties, cost-effectiveness, and use of solar energy, MoS_2 has been identified as a renowned metal free photocatalyst for the degradation of organic contaminants. The layered MoS_2 has effectively synthesized and reported that the metal free photocatalyst exhibited photocatalytic activity under visible light irradiation for the elimination of organic contaminants from aqueous solution [16]. MoS_2 has high photocatalytic activity and inexpensive that it has become preferable in water purification.

In this study, MoS_2 was synthesised through the hydrothermal method as fine powder to be used in the photocatalytic degradation of MB under fluorescent light via response surface methodology by using Design Expert Software of Box-Behnken design. To the best of authors' knowledge, there is no study on box Behnken optimisation design on the degradation of MB under fluorescent light by using MoS_2 as photocatalyst. Therefore, this study could pave a way for the development of facile and optimised approaches for the degradation and treatment of organic pollutants, especially dyes.

Materials and Methods

Materials

Methylene blue, 37% hydrochloric acid (HCl), distilled water, deionised water, sodium molybdate (Na_2MoO_4) and 99% Thiourea (H_2NCSNH_2) were purchased from Sigma Aldrich and all the chemicals are of analytical grade.

Instruments

Fourier transform infrared spectroscopy (FTIR) were recorded between 400 cm^{-1} and 4000 cm^{-1} (Model 100 Spectrometer, Perkin Elmer), UV-visible spectroscopy with 200 nm -800 nm of scanning wavelength (model Lambda 750, Perkin Elmer), X-ray diffractometer analysis were conducted with Panalytical model Empyrean X-ray by keeping 2θ = 10°-90° using Cu, Kα radiations (λ= 1.54059 Å). Scanning electron microscopy (model TESCAN, VEGA3) and thermal gravimetry analyser (TGA) was done by using (model NETZSCH TG 209F3) from 200 °C to 900 °C with the heating rate of 10 °C/min.

Preparation of MoS_2

Sodium molybdate dihydrate ($Na_2MoO_4.2H_2O$) of 3 g and 3.8 g of thiourea (H_2NCSNH_2) was added to 80 mL of deionised water and was stirred for 30 min. 1M HCl of 10 mL was added to the solution and then was transferred into a 100 mL of Teflon stainless steel autoclave. Next, it was heated in an oven at 120 °C for the next 24 h. The solution was cooled at room temperature. After that, the solution was centrifuged three times and washed with deionised water. The solution was oven dried at 70 °C for 24 h.

Characterizations of MoS_2

Sodium molybdate dihydrate ($Na_2MoO_4.2H_2O$) of 3g and 3.8g of thiourea (H_2NCSNH_2) was added to 80 mL of deionised water and was stirred for 30 min. 1M HCl of 10 mL was added to the solution and then was transferred into a 100 mL of Teflon stainless steel autoclave. Next, it was heated in an oven at 120 °C for the next 24 h. The solution was cooled at room temperature. After that, the solution was centrifuged three times and washed with deionised water. The solution was oven dried at 70 °C for 24 h.

Photocatalytic activity

The photocatalytic properties of MoS_2 were evaluated by employing MB as a target degradation product. To determine the MB degradation, the MoS_2 powder was first screened. Next, 0.1 g of MB contamination was added to 100 ml volumetric flask. It was then diluted to 1000 ppm followed by 100 ppm to the desired concentration of 10 ppm by using deionized water. 10 ml from 10 ppm stock solution was pipetted into the immersion tube containing the sample. Then, the sample was placed in a photoreactor for approximately 30 min in the dark to reach an equilibrium. Then, the MB containing the sample was treated under the fluorescent light for 1 h. The reacted MB was next filtered by using the syringe filter. By using UV-vis, the final products were analyzed. The MB showed a strong absorption from deep UV-region to 664 nm. A continuous screening was performed without the involvement of photocatalyst, and a control MB was left incubated without the catalyst and treatment.

$$\text{Percentage degradation efficiency (\%)} = \frac{C_0 - C}{C_0} \; x \; 100 \qquad (1)$$

Where, C_o is initial concentration of MB and C is concentration of MB after the photocatalytic degradation at the specific time given [19].

Results and Discussion

Characterization of MoS_2: Fourier transform infrared spectroscopy (FTIR)

Figure 1 shows various peaks in the spectrum on MoS_2 before and after treatment with MB under fluorescent light, within range from 400 cm^{-1} to 4000 cm^{-1}. The characteristic peak of MoS_2 can be confirmed by a strong peak at 539.90 cm^{-1} indicating the presence of Mo-S in MoS_2. The presence of S-S bond at 878.73 cm^{-1}, meanwhile, absorption band at 1603.54 cm^{-1} was caused by Mo-O bonds along with OH group and their stretching vibrations. The absorption band appearred at 3376.76 cm^{-1} was due to the stretching vibration of existing OH group [20].

The FTIR spectrum of MoS_2 after the MB degradation under the fluorescent light treatment. The absorption band for the Mo-S bond at 539.9 cm^{-1}, the peak of S-S bond at 878.73 cm^{-1} and the peak of Mo-O bond at 1603.54 cm^{-1} were not as substantial as they were before the degradation. After the degradation, the absorption band of 3376.76 cm^{-1} for stretching vibration of the existing OH group was no longer visible. Several functional groups of MoS_2 were not observed after the degradation due to the leaching of the samples by repetition of drying and washing.

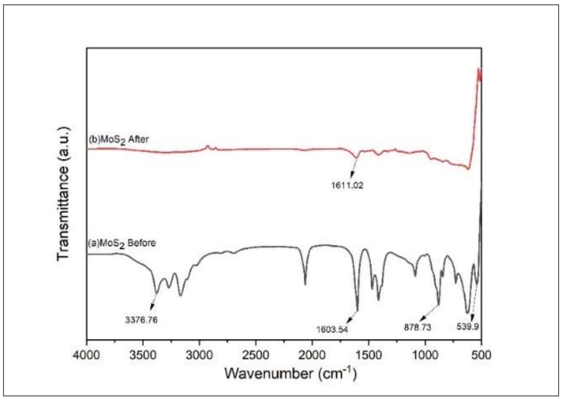

Figure 1. FTIR spectrum of MoS_2 (a) before and (b) after degradation of methylene blue under fluorescent light

UV-visible analysis

As shown in Figure 2, the synthesized MoS_2 nanoparticles showed a strong absorption in UV region with a maximum at 226 nm and a weaker broad absorption in the visible region of 400 nm, which was very similar to that of MoS_2 nanoparticles reported by [21]. Visible light covered the range of approximately 390 nm-700 nm, or 1.8-3.1 eV from the Tauc plot (in-set) the bandgap of MoS_2 was found to be 2.38 eV which revealed that it can be active in the fluorescent light region and effectively degraded the MB.

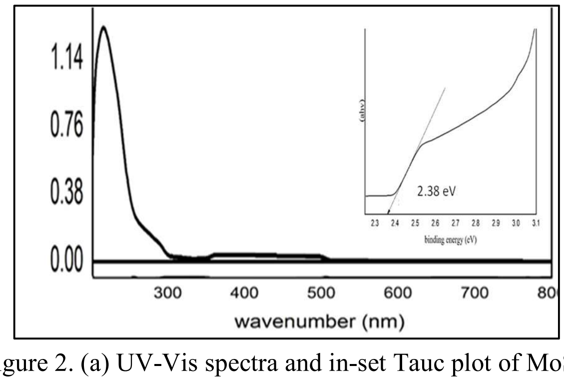

Figure 2. (a) UV-Vis spectra and in-set Tauc plot of MoS_2

X-ray diffraction analysis

Figure 3 indicates diffractogram of MoS_2 exhibited diffraction peaks at 2θ = 14.307°, 32.599°, 40.317°, and 58.235° which can be represented as indices of (002), (100), (103) and (110) of hexagonal phase for the MoS_2 structure, respectively [22]. The crystallinity size calculated was 2.6555Å with the most intense peak. The crystallinity size was calculated by using the Scherrer Equation 2.

$$D = 0.9\ \lambda / \beta \cos\theta \tag{2}$$

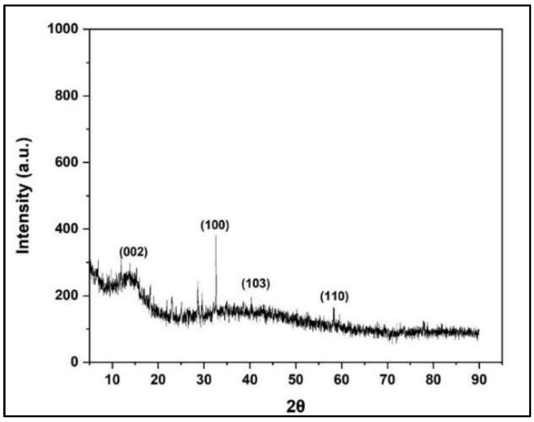

Figure 3. XRD analysis of MoS_2

Morphology analysis

SEM was utilized comprehensively to understand the morphological property of synthesized MoS_2. Figure 4 shows the surface morphology of MoS_2 in flower-like particle. the sheets of MoS_2 stacked together and displayed a 3D cauliflower-like architecture [23]-[24]. Micro-flowers of aggregated MoS_2 nano-sheets were seen in all cases, with no substantial differences. Similar hydrothermally produced materials showed the same morphology [25].

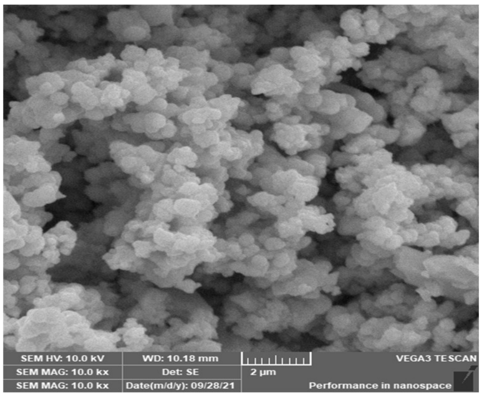

Figure 4. SEM image of MoS_2

Thermogravimetric analysis

Figure 5 illustrates product composition of MoS_2. At the temperature ranging from 200 °C to 470 °C, the TG curve can be interpreted to show three phases of decomposition. MoS_2 exhibited significant initial weight loss at about 200 °C, which could be attributed to water evaporation because of the sample not being completely dried. Furthermore, at 270 °C, MoS_2 lost weight, which could be attributed to oxidation of MoS_2 into MoO_3. The continuous weight loss in the second phase of TG curve decomposition was caused by the thermal decomposition of the organic group. Beyond 400 °C in the final stage, this was primarily due to MoS_2 burned in the air [26].

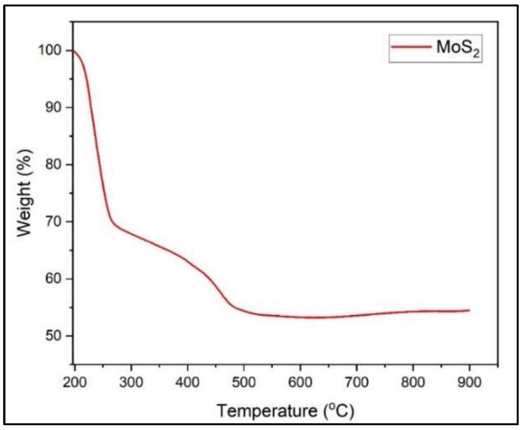

Figure 5. TGA analysis of MoS_2

Photocatalytic activity study: The photocatalytic activity of MoS_2 and methylene blue

The degradation of MB was determined by the screening study of MoS_2 powder. The degradation study of MB was then conducted by using UV-Vis spectroscopy with a maximum absorption at wavelength of 664 nm. The MB underwent treatment for 1 h after incubating for 30 min to reach an equilibrium. Figure 6 shows the UV-Vis spectra of MB before photodegradation and after photodegradation with MoS_2 under the fluorescent light in 120 min. After the photodegradation, the intensity of MB maximum peak decreased showing that MoS2 had successfully degraded MB.

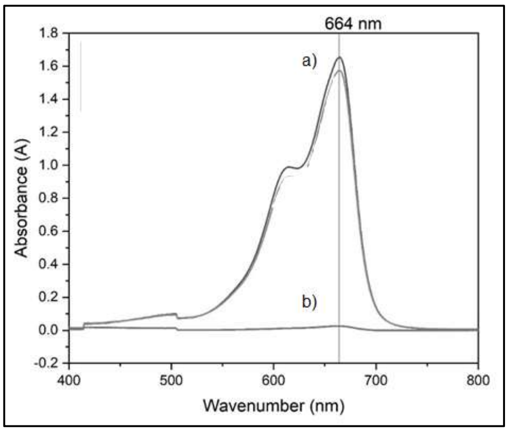

Figure 6. UV-vis spectrum of screening study of methylene blue a) before photodegradation b) after photodegradation

The response surface study

The data were analyzed and interpreted by using Design Expert Software for response surface methodology. Table 2 represents the design experiment of various variables together with experimental and predicted degradation percentage for three-factor-three-level of Box-Behnken design (BBD) response surface analysis for the degradation of MB. The effective parameters studied included A: weight loading (A: 1 mg, 8 mg and 15 mg), B: contact time (B: 5 min, 62.5 min and 120 min) and C: pH value (C: pH 4, pH 6.5 and pH 9). A total of 17 experiments were obtained at random to study the optimized parameters and maximize the photocatalytic degradation of MB. The experimental values are tabulated in Table 2.

Table 2. Response surface analysis for design experiment of degradation of MB

Std	Weight Loading (mg)	Contact Time (min)	pH	Degradation (%)
1	1	5	6.5	24.04
2	15	5	6.5	99.00
3	1	120	6.5	52.99
4	15	120	6.5	99.93
5	1	62.5	4	37.06
6	15	62.5	4	99.23
7	1	62.5	9	47.94
8	15	62.5	9	99.08
9	8	5	4	94.03
10	8	120	4	99.57
11	8	5	9	97.44
12	8	120	9	99.00
13	8	62.5	6.5	99.43
14	8	62.5	6.5	97.87
15	8	62.5	6.5	95.73
16	8	62.5	6.5	94.59
17	8	62.5	6.5	94.24

The data pointed out in Figure 7 was compared to a straight line, indicating that the residual was normally distributed. The residual versus predicted response value, on the contrary, placed the implication of constant variance to the test. The plot should be in random scatter with a constant range of residuals within the residual range [25].

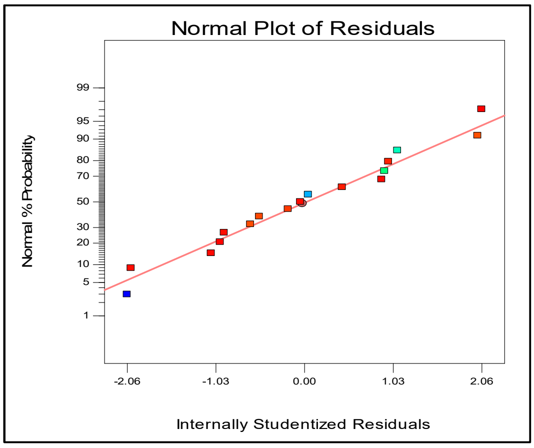

Figure 7. The normal percentage probability and internally studentized residual graph

ANOVA was used to determine the statistical significance of the BBD model. Table 3 summarizes the ANOVA results. The results showed that the acquired models can be used to successfully navigate the design space. The correlation coefficients of R^2 and adjusted R^2 were both high, with values of 0.9904 and 0.9779 demonstrating a close fit between the predicted and experimental values, respectively. The model *F*-value of 79.85 and *p*-values less than 0.0001 implied that the model was significant. Values of *"*Prob>*F"* less than 0.0500 suggested that the model terms were significant. Thus, in this case, *A*, *B*, *AB*, and A^2 were significant model terms. From the ANOVA analysis, the Lack of Fit *F*-value" was not significant. As can be seen in Table 3, the obtained *F* values for effect of weight loading, contact time and pH value were 476.46, 11.78 and 1.59, respectively, showing that the weight loading was the most significant parameter, followed by contact time and pH value. By comparing the interactive model term, *AB* had the highest *F* value of 13.52, followed by *AC* with 2.10 and BC with 0.27, indicating that the interaction of *AB* was the most significant towards photodegradation of MB.

The different MoS_2 weight loading in MB towards photocatalytic reactions are presented in Figure 8(a). It could be seen that when the weight loading of MoS_2 increases, it will increase the number of photocatalyst's active sites that were exposed to the fluorescent light. However, when weight loading exceeded 11.5 mg, the degradation decreased due to the agglomeration of the photocatalyst [27]. According to Figure 8(b), the effect of contact time of MoS_2 on the degradation efficiency of MB was studied within the range of 5 min-120 min during the photocatalytic degradation under the fluorescence light utilizing a photoreactor. It showed that the increase in contact time to 120 min elevated the efficiency of degradation. The first increase in contact time enhanced the efficiency of degradation because actives site of MoS_2 were still vacant and more photodegradation could occur rapidly. Figure 8(c) reveals that the maximum degradation took place within the pH value range of pH 6.5-pH 9 [28].

The response surface plot in three dimensional was plotted to show the interaction between the two parameters towards the photodegradation of MB. In this approach, two parameters were varied within the experimental ranges, while another one parameter was kept constant. The 3-D surface plot of photodegradation of MB as a function of weight loading and contact time is shown in Figure 9.

Table 3. Analysis of variance

Source	df	SS	MS	*F*	*p*	Remark
Model	9	10430.16	1158.91	79.85	<0.0001	significant
Weight Loading, *A*	1	6915.47	6915.47	476.46	<0.0001	
Contact Time, *B*	1	170.94	170.94	11.78	0.0110	
pH, *C*	1	23.02	23.02	1.59	0.2483	
AB	1	196.28	196.28	13.52	0.0079	
AC	1	30.42	30.42	2.10	0.1910	
BC	1	3.96	3.96	0.27	0.6175	
A^2	1	3076.81	3076.81	211.99	<0.0001	
B^2	1	0.52	0.52	0.035	0.8559	
C^2	1	9.32	9.32	0.64	0.4493	
Residual	7	101.60	14.51			
Lack of fit	3	81.87	27.29	5.53	0.0659	Not significant
Pure error	4	19.73	4.93			
Total	16	10531.76				

DF degree of freedom of different source, SS sum of square, MS mean of square, *F* degree of freedom, *P* probability.
*R^2 = 0.9904 and adj-R^2 = 0.9779

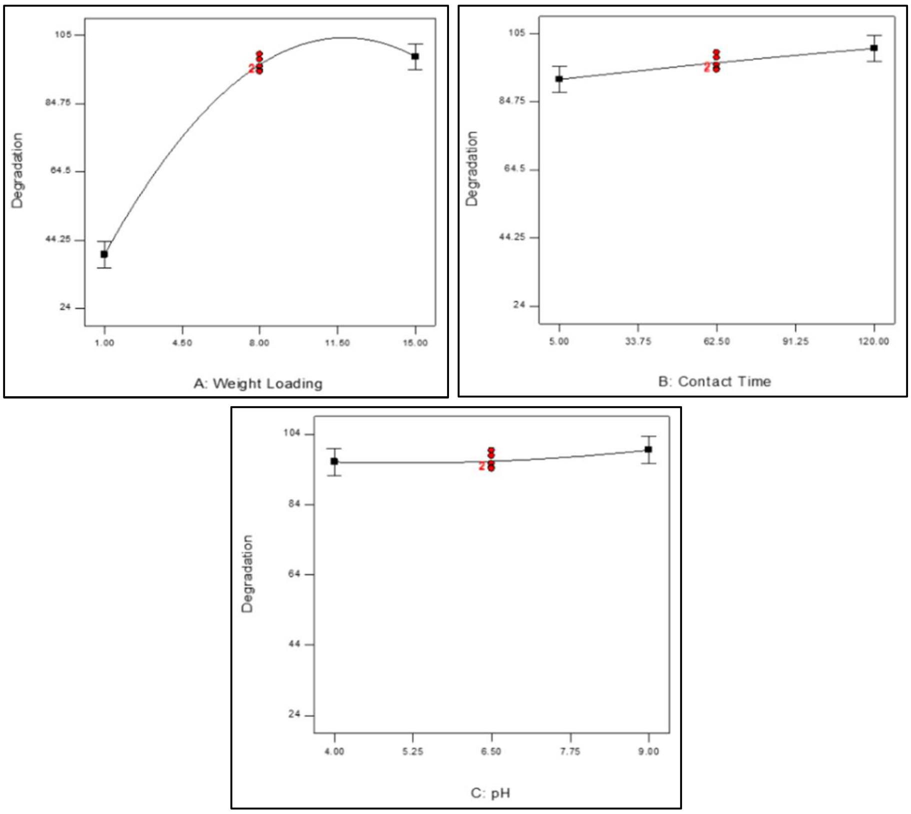

Figure 8. (a) One factor plots of degradation versus weight loading, A (b) degradation and contact time, B plotted graph (c) percentage degradation of methylene blue versus pH, C.

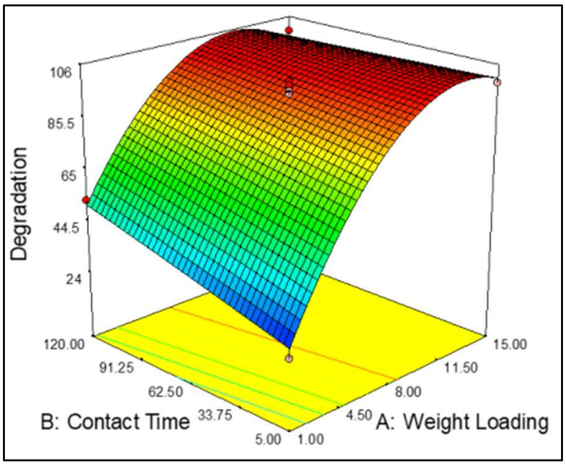

Figure 9. 3-D surface plot of two parameters toward degradation of methylene blue for weight loading and contact time

The pH value was kept constant at pH 6.5. The straight line of the contour plot indicated the interaction of weight loading and contact time. As the weight loading increased along with contact time, the percentage degradation of MB increased. However, as the contact time increased but the weight loading decreased, the percentage degradation was low. This showed that weight loading had significantly contributed to the degradation of MB. Nevertheless, pH value did not play a significant role in the degradation of MB by using MoS_2 under the fluorescent light.

Conclusion

Based on the overall result and discussion, it can be concluded that the MoS_2 was successfully synthesised by the hydrothermal method. The synthesised MoS_2 was characterised by using FTIR, UV-vis solid, XRD, SEM and TGA analyses. The characterisation results clearly revealed that a flower-like MoS2 has been successfully synthesised. For the photocatalytic study of MB, the optimum condition for photodegradation of methylene blue by using MoS_2 were observed under pH 6.5 for MB with MoS_2 weight loading of 15 mg which ran for 120 min which had the highest percentage degradation with value 99.93% as compared to other samples under the fluorescent light. As observed, the most effective parameters in the degradation of MB were weight loading followed by the contact time and pH value.

Acknowledgement

We acknowledge School of Chemistry and Environment, Faculty of Applied Science UiTM Negeri Sembilan for the facilities that have been provided for the research. In addition, we acknowledge Fundamental Research Grant Scheme (FRGS/1/2022/STG05/UITM/02/12) from Ministry of Higher Education Malaysia and (Geran Insentif Penyeliaan [600-RMC/GIP 5/3 (103/2022) by Universiti Teknologi MARA Malaysia for financial support**.**

References

1. Selvam, R., Durai, N., Mubarakali, H., and Vasanthy, M. (2018). Treatment of fabric dyeing industry effluent employing low-cost material: an eco- friendly approach. *International Journal of Basic and Applied Research,* 8(9): 1298-1307.
2. Bentahar, S., Dbik, A., El Khomri, M., El Messaoudi, N., and Lacherai, A. (2018). Removal of a cationic dye from aqueous solution by natural clay. *Groundwater for Sustainable Development,* 6: 255-262.
3. Berradi, M., Hsissou, R., Khudhair, M., Assouag, M., Cherkaoui, O., El Bachiri, A., and El Harfi, A. (2019). Textile finishing dyes and their impact on aquatic environments. *Heliyon,* 5(11): e02711.
4. Krishnamoorthy, R., Choudhury, A. R., Jose, P. A., Suganya, K., Senthilkumar, M., Prabhakaran, J., Gopal, N. O., Choi, J., Kim, K., Anandham, R., and Sa, T. (2021). Long-term exposure to azo dyes from textile wastewater causes the abundance of saccharibacteria population. *Applied Sciences (Switzerland)*, 11(1):1-8.
5. Almaamary, E. A. S., Abdullah, S. R. S., Hasan, H. A., Rahim, R. A. A., and Idris, M. (2017). Rawatan metilena biru dalam air sisa menggunakan *Scirpus grossus*. *Malaysian Journal of Analytical Sciences,* 21(1): 182-187.
6. Bodzek, M., and Rajca, M. (2012). Photocatalysis in the treatment and disinfection of water. Part I. Theoretical backgrounds. *Ecology Chemical Engineering Sciences*, 19(4): 489-512.
7. Baharin, S. N. A., Rusmin, R., and Sambasevam, K. P. (2022). Basic concept and application of conducting polymers for environmental protection. *Chemistry Teacher International,* 4(2): 173-183.
8. Singh, P., Shandilya, P., Raizada, P., Sudhaik, A., Rahmani-sani, A., & Hosseini-bandegharaei, A. (2018). Review on various strategies for enhancing photocatalytic activity of graphene-based nanocomposites for water purification. *Arabian Journal of Chemistry,* 3: 1-23.
9. Zhang, L., and Jaroniec, M. (2018). Toward designing semiconductor-semiconductor heterojunctions for photocatalytic applications. *Applied Surface Science*, 430: 2-17.
10. Poorsajadi, F., Sayadi, M. H., Hajiani, M., and Rezaei, M. R. (2022). Synthesis of CuO/Bi_2O_3 nanocomposite for efficient and recycling photodegradation of methylene blue dye. *International Journal of Environmental Analytical Chemistry,* 102(18): 7165-7178.
11. Sanad, M. M., Farahat, M. M., El-Hout, S. I., and El-Sheikh, S. M. (2021). Preparation and characterization of magnetic photocatalyst from the banded iron formation for effective photodegradation of methylene blue under UV and

and visible illumination. *Journal of Environmental Chemical Engineering,* 9(2): 105127.
12. Drmosh, Q. A., Hezam, A., Hendi, A. H. Y., Qamar, M., Yamani, Z. H., and Byrappa, K. (2020). Ternary $Bi_2S_3/MoS_2/TiO_2$ with double Z-scheme configuration as high performance photocatalyst. *Applied Surface Science,* 499: 143938.
13. He, Z., & Que, W. (2016). Molybdenum disulfide nanomaterials: Structures, properties, synthesis and recent progress on hydrogen evolution reaction. *Applied Materials Today,* 3: 23-56.
14. Kumar, R., Ansari, S. A., Barakat, M. A., Aljaafari, A., and Cho, M. H. (2018). A polyaniline@MoS_2-based organic–inorganic nanohybrid for the removal of Congo red: adsorption kinetic, thermodynamic and isotherm studies. *New Journal Chemistry*, 42:18802-18809.
15. Chaudhary, N., Raj, K., Harikumar, A., Mittal, H., and Khanuja, M. (2020). Comparative study of photocatalytic activity of hydrothermally synthesized ultra-thin MoS_2 nanosheets with bulk MoS_2. *AIP Conference Proceedings*, 2276: 20030.
16. Vattikuti, S. V. P., and Shim, J. (2018). Synthesis, characterization and photocatalytic performance of chemically exfoliated MoS_2. *IOP Conference Series: Materials Science and Engineering*, 317(1): 1-5.
17. Abdulhameed, A. S., Mohammad, A. K. T., and Jawad, A. H. (2019). Application of response surface methodology for enhanced synthesis of chitosan tripolyphosphate/TiO_2 nanocomposite and adsorption of reactive orange 16 dye. *Journal of Cleaner Production,* 232: 43-56.
18. Chen, J., and Zhang, P. (2006). Photodegradation of perfluorooctanoic acid in water under irradiation of 254 nm and 185 nm light by use of persulfate. *Water Science and Technology*, 54(11-12): 317-325.
19. Ibukun, O., Evans, P. E., Dowben, P. A., and Jeong, H. K. (2019). Titanium dioxide-molybdenum disulfide for photocatalytic degradation of methylene blue. *Chemical Physics,* 525:110419.
20. Chaudhary, N., Khanuja, M., Abid, and Islam, S. S. (2018). Hydrothermal synthesis of MoS_2 nanosheets for multiple wavelength optical sensing applications. *Sensors and Actuators, A: Physical*, 277(2010): 190-198.
21. Chen, Y., Tan, L., Sun, M., Lu, C., Kou, J., and Xu, Z. (2019). Enhancement of photocatalytic performance of TaON by combining it with noble-metal-free MoS_2 cocatalysts. *Journal of Materials Science,* 54(7): 5321-5330.
22. Yang, J., Ye, M., Han, A., Zhang, Y., and Zhang, K. (2019). Preparation and electromagnetic attenuation properties of MoS_2–PANI composites: a promising broadband absorbing material. *Journal of Materials Science: Materials in Electronics,* 30(1): 292-301.
23. Peng, W., Wang, W., Han, G., Huang, Y., and Zhang, Y. (2020). Fabrication of 3D flower-like MoS2/graphene composite as high-performance electrode for capacitive deionization. Desalination, 473(August 2019), 11: 4191.
24. Ariyanta, H. A., Ivandini, T. A., and Yulizar, Y. (2021). A novel way of the synthesis of three-dimensional (3D) MoS_2 cauliflowers using allicin. *Chemical Physics Letters,* 767: 138345.
25. Koh, P. W., Yuliati, L., and Lee, S. L. (2017). Kinetics and optimization studies of photocatalytic degradation of methylene blue over Cr-doped TiO_2 using response surface methodology. *Iranian Journal of Science and Technology, Transaction A: Science,* 43(1): 95-103.
26. Bahuguna, A., Kumar, S., Sharma, V., Reddy, K. L., Bhattacharyya, K., Ravikumar, P. C., and Krishnan, V. (2017). Nanocomposite of MoS_2-RGO as facile, heterogeneous, recyclable, and highly efficient green catalyst for one-pot synthesis of indole alkaloids. *ACS Sustainable Chemistry & Engineering,* 5(10): 8551-8567.
27. Norsham, I. N. M., Sambasevam, K. P., Shahabuddin, S., Jawad, A. H., and Baharin, S. N. A. (2022). Photocatalytic degradation of perfluorooctanoic acid (PFOA) via MoS_2/rGO for water purification using indoor fluorescent irradiation. *Journal of Environmental Chemical Engineering,* 10(5): 108466.
28. Taghvaei, H., Farhadian, M., Davari, N., and Maazi, S. (2017). Preparation, characterization and photocatalytic degradation of methylene blue by Fe^{3+} doped TiO_2 supported on natural zeolite using

response surface methodology. *Advances in Environmental Technology,* 3(4): 205-216.